Supporting Information

Antimicrobial and Anti-Inflammatory Effects of Polyethyleneimine-Modified Polydopamine Nanoparticles on a Burn-Injured Skin Model

Sadman Sakib,[1, †] *Nesha May O. Andoy,*[2, †] *Jessica Y. C. Yang,*[2] *Anna Galang,*[2,3] *Ruby May A. Sullan,* [2,3]* *and Shan Zou*[1]*

[1]Metrology Research Centre, National Research Council Canada, 100 Sussex Drive, Ottawa, Ontario, K1N 5A2, Canada [2]Department of Physical and Environmental Sciences, University of Toronto Scarborough, 1065 Military Trail, Toronto, ON, M1C 1A4 Canada; [3]Department of Chemistry, University of Toronto, 80 St. George St., Toronto, ON, M5S 3H6, Canada

I. Characterization of PDNP and PDNP-PEI

Dynamic light scattering (DLS), phase analysis light scattering (PALS), transmission electron microscopy (TEM) and Fourier-transform infrared (FTIR) spectroscopy were used to characterize the polydopamine nanoparticles (PDNPs) and to confirm successful surface functionalization with polyethyleneimine (PEI). Figure S1A (red box plots) shows that the average hydrodynamic size of the particles increased from 85 ± 23 nm (PDNPs) to 205 ± 43 nm after surface modification with PEI (i.e., PDNP-PEI). The increase in size was accompanied by a complete reversal of the measured surface zeta potential—while PDNPs registered an average of −33 ± 4 mV potential, this shifted to more positive values (i.e., +31 ± 4 mV) after PEI immobilization (Figure S1A, blue box plots). The increase in hydrodynamic size and reversal of the surface zeta potential indicates the presence of high-density positively charged amine groups characteristic of bPEI, confirming successful surface functionalization. In addition to DLS and PALS measurements, TEM was used to visualize the morphology of the nanoparticles (Figure S1B). Figure S1B shows that only the polydopamine core (and not the PEI coating) can be observed under TEM (Figure S1B). However, surface modification was further confirmed by comparing FTIR spectrum of PDNPs with that of PDNP-PEI. Figure S1C (blue arrow) highlights that after surface modification, additional peaks corresponding to aliphatic ν(C–H) stretching modes at 2940 and 2850 cm^{-1} can be observed on top of the characteristic broad peak between 3000−2500 cm^{-1} for PDNPs. Taken together, these physical characterizations demonstrate that by simply incubating PDNPs with bPEI under basic conditions, PEI-decorated PDNPs can readily form.

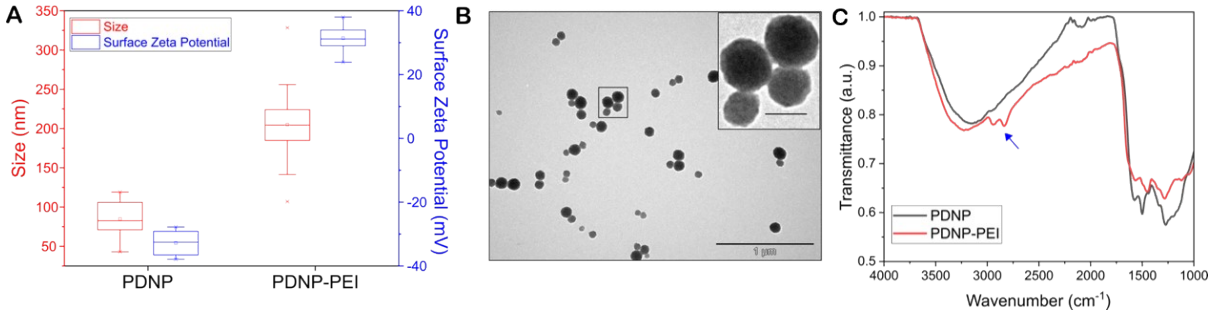

Figure S1 Surface modification of polydopamine nanoparticles (PDNP) with polyethyleneimine (PEI) to create PDNP-PEI. (A) Increase in the hydrodynamic size of PDNPs (blue) following functionalization with PEI, accompanied by a reversal of surface zeta potential in the presence of PEI. (B) Transmission Electron Microscopy (TEM) image illustrating the structure of PDNP-PEI. (C) FTIR spectrum of PDNPs (black) and PDNP-PEI (red).

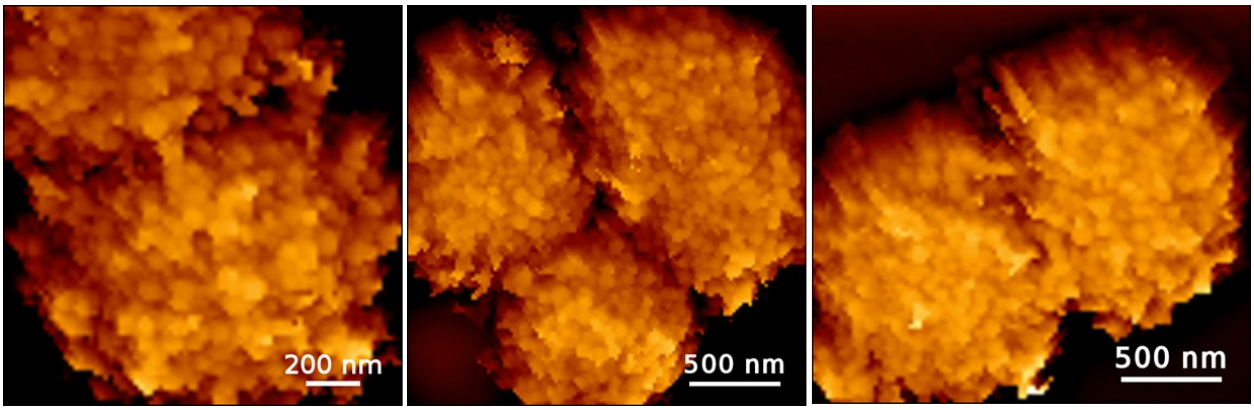

Figure S2 PDNP-PEI binds the surface of a Gram-positive bacteria: AFM images of *S. epidermidis* (OD_{600nm} = 0.01) immobilized on polycarbonate (PC) membrane after 30-min incubation with PDNP-PEI (25 µg/mL) in 10 mM Bicine buffer pH 7.5.

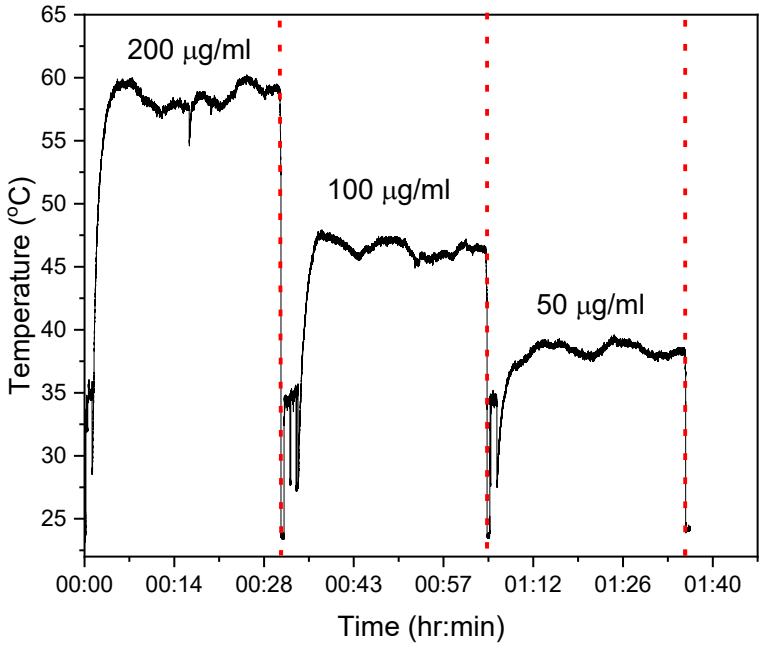

Figure S3 Laser-induced photothermal activity of PDNP-PEI: Solution temperature profile of different concentrations of PDNP-PEI in 10 mM Bicine buffer pH 7.5. A CW 808nm laser (7 W cm^{-2}) was used to irradiate the 100 μL PDNP-PEI solution, while a thermal imager was used to record the maximum temperature during laser irradiation.

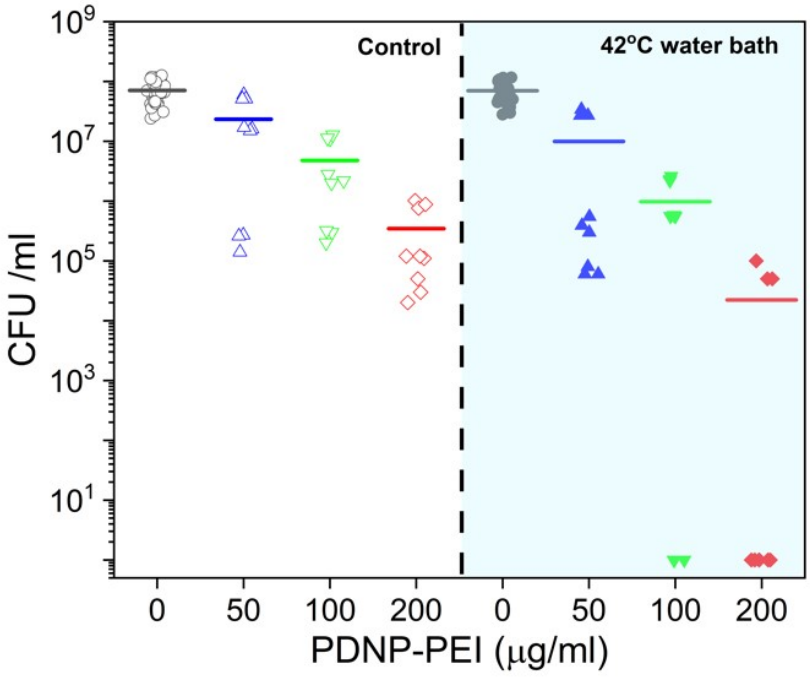

Figure S4 Antimicrobial activity of PDNP-PEI + heat treatment: Number of viable bacteria left after *S. epidermidis* (OD_{600nm} = 0.01) was mixed with increasing concentrations of PDNP-PEI for 30 min, in 10 mM Bicine buffer pH 7.5 and heated at 42 °C using a water bath.

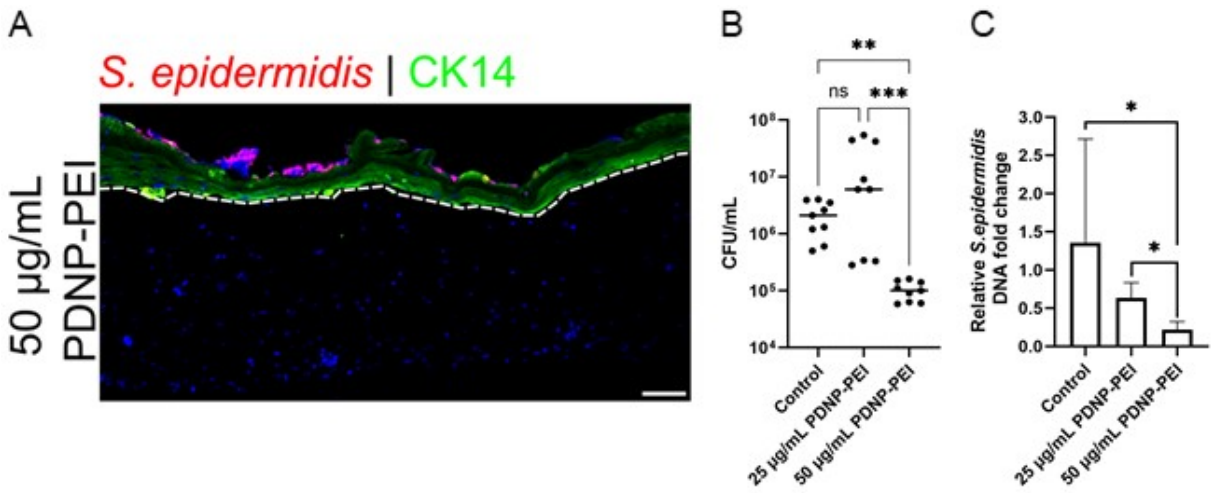

Figure S5 PDNP-PEI displayed anti-biofilm activity only at 50 µg/mL post laser irradiation. (A) Immunofluorescence imaging of biofilm 48 h after treatment. Biofilm shown in red via immunohistochemistry of *S. epidermidis*. CK14^{+ve} keratinocytes (green) and white dash line delineate the epidermis and dermis. Hoechst (blue) is used as a nuclear stain. Scale bar = 100 µm. (A) Number of viable bacteria on skin after PDNP-PEI treatment post laser mediated heating. (B) Relative fold change of *S. epidermidis* DNA expression after PDNP-PEI treatment. Values on each graph are shown as mean ± SD of at least five independent experiments. Statistical significance was determined with one-way ANOVA. *P < 0.05; **P < 0.01; ***P < 0.001; and ****P < 0.0001.

II. Loading of PDNP-PEI with rifampicin enhances bactericidal and anti-biofilm activity

We leveraged PDNP's ability to bind to other molecules through multiple interactions via its surface functional groups (i.e., phenolic hydroxyls, amines, and quinones).[S1] PDNPs have been extensively studied as a drug nanocarrier and loaded with various cargoes such as anticancer drugs (doxorubicin, camptothecin, cisplatin), photosensitizers (chlorin e6, indocyanine green), as well as antibiotics (ciprofloxacin, vancomycin, tetracycline).[S2-3] Rifampicin is a highly effective antibiotic against *S. epidermidis* (Figure S6).

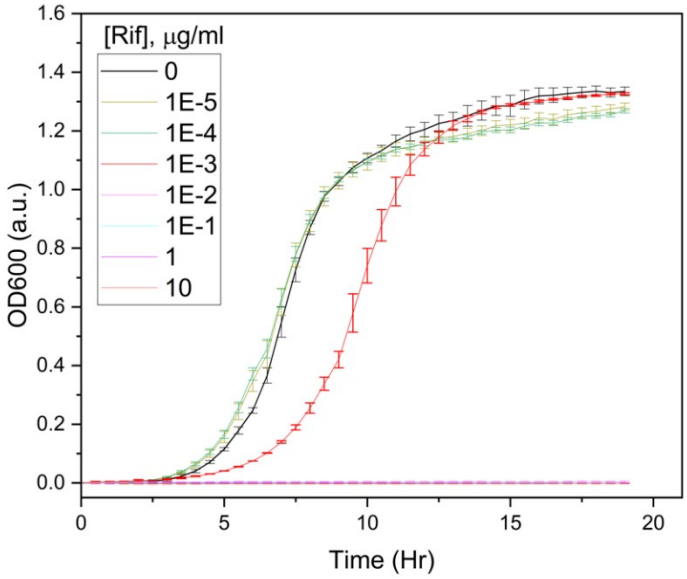

Figure S6 Antimicrobial activity of rifampicin: Growth of *S. epidermidis* in TSB media, at 37°C, in the presence of increasing concentrations of Rifampicin.

After PDNP-PEI was incubated with rifampicin overnight, the drug-loaded nanoparticles were removed via centrifugation and the amount of rifampicin remaining in solution was determined using UV-Vis spectroscopy. Figure S7A shows the absorption spectrum of the rifampicin solution before (**black**) incubation with PDNP-PEI (1:1 w/w) and the absorption spectrum of the same Rifampicin solution after the removal of nanoparticles via centrifugation (**blue**). The *difference* in

the absorption spectra represents the amount of rifampicin that was loaded into the nanoparticles (Figure S7A red arrow). The absorbance at 475 nm from these spectra was then used to calculate the total amount of rifampicin that got loaded into the nanoparticle, from which 19 ± 9 % (w/w) drug loading capacity was calculated for PDNP-PEI. The hydrodynamic size (237 ± 50 nm) and surface zeta potential (30 ± 3 mV) of the drug-loaded nanoparticles (i.e., PDNP-PEI-Rif, n = 5) are similar to those of PDNP-PEI, showing that drug loading did not alter the physical properties of the nanoparticles. We further characterize the efficiency of cargo release with and without laser-irradiation to determine whether the laser-induced heating of PDNP could induce drug release, as we have previously observed for drug-loaded PDNP using other antibiotics.[S4] Figure S7B shows that compared to non-irradiated nanoparticle solution, 30-min laser treatment resulted in almost double the amount of rifampicin released from PDNP-PEI-Rif: 1.7 % (Laser-induced release) vs. 0.9 % (Passive release).

We then evaluated the antimicrobial activity of rifampicin-loaded PDNP-PEI-Rif against planktonic *S. epidermidis*. The bacteria were pre-exposed to increasing concentrations of PDNP-PEI-Rif for 10 min in 10 mM Bicine buffer, before 10 uL of each solution was diluted to 200 uL with TSB, and planktonic growth was monitored. Bacterial growth was already inhibited at concentrations as low as 5 μg/mL after 18 h (Figure S7C). Moreover, almost complete growth inhibition occurred when *S. epidermidis* was incubated with ≥ 10 μg/mL PDNP-PEI-Rif. This reduction in the number of viable bacteria was achieved even without laser irradiation, making antibiotic-loaded PDNP-PEI more effective as an antimicrobial agent than nanoparticles without their antibiotic cargo. Comparing to free antibiotic shows that the antibacterial effect of PDNP-PEI-Rif could be attributed to their drug cargo as rifampicin is very effective against *S. epidermidis*.

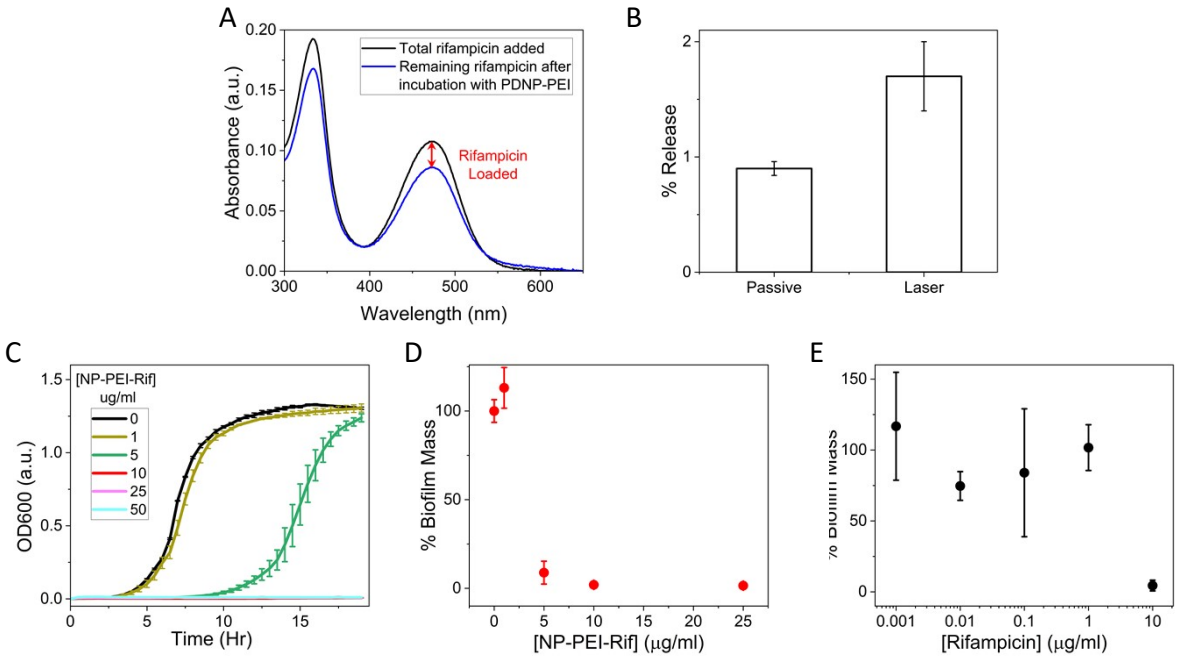

Figure S7. Rifampicin loading, antimicrobial and antibiofilm activities of PDNP-PEI-Rif. (A) The absorption spectrum of rifampicin before incubation with PDNP-PEI (black) and the absorption spectrum of the same rifampicin solution after the removal of the nanoparticles (blue). The difference in absorbance of rifampicin (red arrow) shows the amount of antibiotics loaded into the nanoparticles. (B) Amount of drug released from PDNP-PEI-Rif after 30 min incubation, with (Laser) and without (Passive) laser irradiation. (C) Growth inhibition of *S. epidermidis* in response to increasing concentrations of PDNP-PEI-Rif. Biofilm mass formed after 24-hr growth, following a 10-minute incubation with (D) PDNP-PEI-Rif and (E) Rifampicin alone, with nanoparticles and antibiotics removed via filtration.

Next, we tested the ability of drug-loaded PDNP-PEI to prevent biofilm formation. One of the main advantages of PDNP-PEI as a drug nanocarrier is its ability to bind to the bacterial surface, providing the added benefit of localized and sustained availability of drug molecules. To test this hypothesis, we pre-exposed *S. epidermidis* to different concentrations of PDNP-PEI-Rif for only

10 min before isolating the bacteria via filtration using a 0.8 μm polycarbonate (PC) membrane. This filtration step washes away any drug-loaded nanoparticles that did not bind to the bacterial surface during incubation. As a control, we also exposed *S. epidermidis* to free rifampicin for 10 min before filtration—to directly compare how the bacterial-adhering, drug-loaded PDNP-PEI performs against the free drug when the exposure time is limited. Figure S7D shows that biofilm formation was inhibited by more than 90% when bacteria were pre-exposed to 5 μg/ml PDNP-PEI-Rif (i.e., ~1 μg/mL total rifampicin loaded). In contrast, when *S. epidermidis* was pre-exposed to a free antibiotic, ~10 μg/mL of rifampicin was needed to prevent biofilm formation (Figure S7E).

These results demonstrate that the ability of PDNP-PEI for drug loading (Figure S7A) and its ability to bind to the bacterial surface (Figure 1A) allow for sustained availability of rifampicin, locally concentrating the antibiotic close to the bacteria and preventing biofilm growth at nanoparticle concentrations as low as 5 μg/ml (with ~1 μg/ml antibiotic). Conversely, incubating with free drug molecules dramatically decreased bioavailability after filtration, as unbound antibiotics were washed away, allowing biofilm growth even at very high antibiotic concentrations (i.e., ~1000 × MIC). These results emphasize the need for sustained bioavailability of antibiotics, which normally requires administering very high doses of drug molecules—leading to antibiotic overuse and contributing to the development of antibiotic resistance.

In addition, though we only show here that PDNP-PEI and PDNP-PEI-Rif are effective against *S. epidermidis* (planktonic and biofilms), this platform can readily be adapted to target other bacteria: (i) PEI being cationic can bind the surface of both Gram-positive and Gram-negative bacteria, (ii) Rifampicin is also active against other bacteria, and (iii) laser-induced heating is also

effective in killing common human pathogens. Furthermore, the modular and highly tunable nature of PDNP towards cargo loading and surface functionalization makes the PDNP-Polymer-Drug platform easily adaptable for applications towards other bacteria. Different bacterial targeting polymers (e.g., antimicrobial peptides, chitosan, antibodies, etc.) can readily be attached to the surface of PDNP, which can then be loaded with other antimicrobial molecules, to target either a broad spectrum or specific bacterial species.

References

S1. Liu, Y.; Ai, K.; Lu, L. Polydopamine and Its Derivative Materials: Synthesis and Promising Applications in Energy, Environmental, and Biomedical Fields. *Chem. Rev.* **2014**, *114*, 5057–5115.

S2. Batul, R.; Tamanna, T.; Khaliq, A.; Yu, A. Recent progress in the biomedical applications of polydopamine nanostructures. *Biomater. Sci.* **2017**, *5*, 1204–1229.

S3. Jin, A.; Wang, Y.; Lin, K.; Jiang, L. Nanoparticles modified by polydopamine: Working as "drug" carriers. *Bioact. Mater.* **2020**, *5*, 522–541.

S4. Patel, M.; Andoy, N.M.O.; Tran, S.M.; Jeon, K.; Sullan, R.M.A. Different drug loading methods and antibiotic structure modulate the efficacy of polydopamine nanoparticles as drug nanocarriers. *J. Mat. Chem. B.* **2023**, *11*, 11335-11343.